Estimation of optical constants from multiple-scattered light using approximations for single particle scattering characteristics

Maria A. Velazco-Roa and Suresh N. Thennadil*

School of Chemical Engineering and Advanced Materials, University of Newcastle upon Tyne, Newcastle upon Tyne, NE7 7SR, United Kingdom

**Corresponding author: s.n.thennadil@ncl.ac.uk*

The inversion of multiple-scattered light measurements to extract the optical constant (complex refractive index) is computationally intensive. A significant portion of this time is due to the effort required for computing the single particle characteristics (absorption and scattering cross-sections, anisotropy factor and the phase function). This paper investigates approximations for computing these characteristics so as to significantly speed up the calculations without introducing large inaccuracies. Two suspensions of spherical particles viz. polystyrene and poly(methyl methacrylate) were used for this investigation. It was found that using the exact Mie theory to compute the absorption and scattering cross-sections and the anisotropy factor with the phase function computed using the Henyey-Greenstein approximation yielded the best results. Analysis suggests that errors in the phase functions and thus in the estimated optical constants depend mainly on how closely the approximations match the Mie phase function at small scattering angles.

OCIS codes: 290.3030, 290.4020, 290.4210, 290.5820, 290.5825, 290.5850, 290.7050.

1. Introduction

Previously [1], a method to extract the optical constants n(λ) and k(λ) from multiple-scattered light was developed and applied to suspensions of spherical polystyrene latex particles. This method consisted of inverting total diffuse reflectance and transmittance measurements collected with an integrating sphere set-up using the adding-doubling method to solve the radiative transfer equation (RTE) combined with the exact Mie theory to describe single particle absorption and scattering characteristics.

The RTE for light propagation through a slab is given by [2],

$$\frac{dI(\mathbf{r},\hat{\mathbf{s}})}{ds} = -\mu_t I(\mathbf{r},\hat{\mathbf{s}}) + \frac{\mu_s}{4\pi}\int_{4\pi} p(\mathbf{s},\hat{\mathbf{s}}) I(\mathbf{r},\hat{\mathbf{s}}) d\omega \tag{1}$$

where $I(\mathbf{r},\hat{\mathbf{s}})$ is the specific intensity at a point $\mathbf{r}$ with radiation along the direction $\hat{\mathbf{s}}$, μ_t (= μ_s + μ_a) is the bulk extinction coefficient, μ_s is the bulk scattering coefficient and μ_a is the bulk absorption coefficient and $p(\mathbf{s},\hat{\mathbf{s}})$ is the phase function which is a measure of the angular distribution of the scattered light. The bulk scattering and absorption coefficients for a suspension of monodisperse particles in water are given by:

$$\begin{aligned} &\mu_a(\lambda) = \mu_{a,p}(\lambda) + \mu_{a,w}(\lambda); \quad \mu_{a,p}(\lambda) = \rho\sigma_a(\lambda); \\ &\mu_{a,w}(\lambda) = \frac{4\pi k_w(\lambda)(1-c)}{\lambda}; \quad \text{and} \quad \mu_s(\lambda) = \rho\sigma_s(\lambda) \end{aligned} \tag{2}$$

where σ_a, σ_s and ρ are respectively the absorption and scattering cross-sections and number density of the particles, λ is the wavelength of the incident beam, k_w is the imaginary part of the

complex refractive index of water and c is the volume fraction of particles in the sample. For spherical particles, if the complex refractive index and particle size are known, the absorption and scattering cross-sections can be calculated exactly using Mie theory and if the number density is known, the bulk scattering and absorption coefficients for the particles can be computed. Then the RTE can be solved using the adding-doubling method with appropriate boundary conditions [3]. In our case, the complex refractive index of the particles is unknown and can be found by iteratively solving Eq. (1) to generate total diffuse reflectance (R_{cal}) and transmittance (T_{cal}) and comparing these values with experimental measurements (R_{meas} and T_{meas}) such that the following function is minimised [1]:

$$\sum = \mathrm{abs}(R_{meas} - R_{cal}) + \mathrm{abs}(T_{meas} - T_{cal}) \tag{3}$$

At each iteration step, the adding-doubling algorithm to solve the RTE requires as input μ_a, μ_s and the phase function which are computed using Mie theory. The inversion methodology is computationally intensive and it can take a few hours of iterations to invert one sample (over a range of wavelengths) to a desired convergence. Thus approximations which significantly speed up the calculations without introducing large inaccuracies will be desirable. The steps in the iterations that involve the computation of μ_a, μ_s and the phase function through Mie calculations take a significant portion of the computational time. The reduction of computational effort for this part of inversion scheme is investigated in this paper. In order to avoid the complications involved in accounting for inter-particle interactions, in this study the concentrations are kept below the levels indicated by the analysis carried out previously [1] which indicated that above a weight fraction of about 0.025, the refractive index values show a concentration dependence when the current inversion scheme is used. Thus the focus is on systems where the concentration

is sufficiently high for multiple scattering effects to be significant without being affected by inter-particle interactions.

2. Approximations to single particle scattering characteristics

To speed up the calculations, two approaches were tried. One was to replace the Mie calculations with the Rayleigh-Gans-Debye [4] approximation to calculate the absorption and scattering cross-sections and the phase function. The second approach was to calculate the absorption and scattering cross-sections and the anisotropy parameter (g) exactly using Mie theory and use approximations to the phase function which are written in terms of g. The Henyey-Greenstein [5] and the modified Henyey-Greenstein [6, 7] approximations were used in this study.

(a) Rayleigh-Gans-Debye (RGD) approximation

In the RGD approximation, the absorption and scattering cross-sections are given by [4, 8],

$$\sigma_a(\lambda) = \frac{4\pi n(\lambda)k(\lambda)V_p}{\lambda} \tag{4}$$

and

$$\sigma_{sca} = 2\pi(\hat{n}-1)^2\left\{\frac{5}{2}+2x^2-\frac{\sin 4x}{4x}-\frac{7}{16x^2}(1-\cos 4x)+\left(\frac{1}{2x^2}-2\right)(\gamma+\log 4x-Ci[4x]\right\} \tag{5}$$

where V_p is the volume of the particle, $\hat{n}$ is the real part of the relative refractive index, γ is the Euler's constant and Ci is the cosine integral $Ci(x) = -\int_x^\infty \frac{\cos u}{u} du$, $u = 2a\kappa \sin(\theta/2)$, $\kappa = 2\pi/\lambda_o$, $x = \kappa a$ is the size parameter, a is the radius of the particle, θ is the scattering angle and λ_0 is the wavelength in vacuum.

For symmetric particles, p(**s**, **s'**) varies only along the scattering angle θ and is given by:

$$p(\mathbf{s},\mathbf{s}') = p(\cos\theta) = \frac{F(\theta, a, \hat{n}, \lambda)}{\sigma_{sca}} \tag{6}$$

The anisotropy factor $g = <\cos\theta>$ is given by:

$$g = <\cos\theta> = \frac{1}{4\pi^2} \frac{\int x^4 (\hat{n}-1)^2 (1-\cos^2\theta) P(\theta) \cos\theta d\theta}{\sigma_{scat}} \tag{7}$$

The phase function gives the angular distribution of light for a single scattering event. To solve the RTE using the adding doubling method (ADD), the angular distribution, which takes multiple scattering into account, is required. This is provided by the re-distribution phase function, which determines the fraction of light scattered from an incident cone with angle θ_i into a cone of with angle θ_j. This function is calculated by averaging the phase function over all possible azimuth angles for fixed angles θ_i and θ_j [3, 9],

$$h(\cos\theta_i, \cos\theta_j) = \frac{1}{2\pi} \int_0^{2\pi} p(\cos\theta_i \cos\theta_j + \sqrt{1-\cos\theta_i{}^2} \sqrt{1-\cos\theta_j{}^2} \cos\phi) d\phi \tag{8}$$

The solution of this equation is not straightforward when a phase function such as the RGD phase function is used. The re-distribution phase function can be calculated using the δ-M method [3, 9-11]. In this method the true phase function, $p(\cos\theta)$ is approximated by a phase function $P^*(\cos\theta)$ consisting of a Dirac delta function and M-1 Legendre polynomials,

$$P^*(\cos\theta) = 2f\delta(1-\cos\theta) + (1-f)\sum_{m=0}^{2M-1}(2m+1)\chi_m^* P_n(\cos\theta) \tag{9}$$

where $P^*(\cos\theta)$ is equivalent to the phase function $p(\cos\theta)$, χ_m^* are the expansion coefficients, f is the fractional scattering into the forward peak. The expansion coefficients are found by matching this equation with the first 2M terms of the true phase function expanded in terms of Legendre polynomials:

$$p(\cos\theta) = \sum_{n=0}^{\infty}(2n+1)\chi_n P_n(\cos\theta) \tag{10}$$

Where the coefficients χ_n are computed from the following expression:

$$\chi_n = \frac{1}{2}\int_0^{\pi} p(\cos\theta)P_n \sin\theta d\theta \tag{11}$$

The first coefficient, χ_0 = 1, because the phase function is normalised to 1 [11]. The following relationship is then obtained:

$$\chi_m^* = \frac{\chi_m - f}{1-f}, m = 0,....,2M-1 \tag{12}$$

Where f is set to χ_{2M}. The re-distribution of the phase function using the δ-M approximation can then be written as [9]:

$$h^*(\cos\theta_i, \cos\theta_j) = 2f\delta(\cos\theta_i - \cos\theta_j) + (1-f)\sum_{m=0}^{2M-1}(2m+1)\chi_m^* P_m(\cos\theta_i)P_m(\cos\theta_j) \quad (13)$$

(b) Phase function approximations

The Henyey-Greenstein phase function approximation is a simple analytical expression which has been used extensively to describe forward scattering and is given by [3, 5, 6]:

$$p_{HG}(\cos\theta) = \frac{1-g^2}{[1+g^2-2g\cos\theta]^{3/2}} \quad (14)$$

For this function we get:

$$f = \chi_m = g^M \quad (15)$$

and χ_m^* is given by:

$$\chi_m^* = \frac{g^n - g^M}{1-g^M} \quad (16)$$

From the last equation it is seen that the calculation of χ_m^* is very simple for this case as integration of the equation (11) to compute χ_m are not required.

The H-G approximation does not describe well the forward or backward scattering peak and it does not have the right limiting behaviour viz. it does not reduce to the Rayleigh scattering phase

function in the Rayleigh regime when $\cos\theta \to 0$. Cornette and Shanks[7] proposed a modified Henyey-Greenstein approximation (H-Gm) which reduces to the Rayleigh phase function when $\cos\theta$ tends to 0. The H-Gm function is given by:

$$p_{HGm}(\cos\theta) = \frac{3}{2}\frac{1-g^2}{2+g^2}\frac{1+\cos^2\theta}{[1+g^2-2g\cos\theta]^{3/2}} \tag{17}$$

In this case, however, the calculation of the expansion coefficients χ_m^* has to be carried out numerically by integrating equation (11). Similarly, for the RGD approximation, the expansion coefficients have to be obtained by numerical integration.

3. Materials and Measurements

Suspensions of polystyrene and poly(methyl methacrylate) latex spheres were used in this study. Polystyrene microspheres suspension of 10% by weight of solids of narrow particle size distributions with coefficient of variance (CV), 3% of mean diameter of 0.45 μm was purchased from Duke Scientific. This was diluted using de-ionised water to 0.075% by weight of solids. PMMA microspheres suspension of 2.7% by weight of solids, and 0.324 μm of mean diameter and 0.015 μm of standard deviation was purchased from Polysciences, Inc. A sample was prepared by dilution to 0.56% by weight of solids. The number density of these suspensions were calculated using the density of de-ionised water at room temperature (25˚C), ρ_{medium} =1g/ml, and the corresponding density of the particles: polystyrene particles, $\rho_{particles}$ = 1.05 g/ml, and PMMA particles $\rho_{particles}$ = 1.19 g/ml. The samples were placed in a special optical glass cuvette of 2mm path length. Total diffuse reflectance and transmittance were measured using an integrating sphere of diameter 150mm (DRA-2500, Varian Instruments) attached to a UV-Vis-

NIR spectrophotometer (Cary 5000, Varian Instruments) in the wavelength region 450 - 1320 nm at 20 nm intervals. Three replicates of each (polystyrene and PMMA) sample were obtained by repeating the sample preparation. For each of these replicates, total diffuse reflectance and transmittance were measured three times, thus obtaining 9 measurements for each sample. The values of $n(\lambda)$ and $k(\lambda)$ reported are the mean over the 9 measurements and the error bars indicate 2 times the standard deviation. The relative complex refractive index, m_r is computed as the ratio of the complex refractive index of the particles to the complex refractive index of water. For these calculations the optical constants for the water, $n_w(\lambda)$ and $k_w(\lambda)$ published by Segelstein [12] were used.

4. Results

The optical constants for polystyrene particles obtained using the inverse adding-doubling method along with the exact Mie theory has been previously published [1]. For PMMA, in this wavelength range, to our knowledge only the real part of the refractive index obtained using refractometer measurements has been published before [13]. Figure 1 shows the real and imaginary parts of the refractive index estimated using the inversion method. In figure 1(a), the $n(\lambda)$ values estimated in this study is compared with the published values of Sultanova *et al* [13]. It can be seen while there are slight differences, the agreement is good considering the different methodologies used to extract the refractive index.

Figures 2 (a) and (c) show the values of $n(\lambda)$ and $k(\lambda)$ of polystyrene particles estimated using the RGD approximation and those obtained using the Mie theory. In figure 2(a), it is seen that the $n(\lambda)$ values estimated using the RGD approximation is slightly though significantly higher than the Mie values between 450 and 900 nm, whereas between 900 nm to 1320 nm the

difference is mostly within experimental error. The error over the wavelength range considered is less than 2% as can be seen from figure 2(b). In figure 2(c), it is seen that the RGD estimates of $k(\lambda)$ are appreciably lower than the Mie estimates over the entire wavelength region considered with errors above 20% over most of the wavelengths considered. Similar trends are seen with the PMMA particles as seen in Figures 3(a) and (b).

Next we consider the effect of approximating the phase functions while the scattering and absorption cross-sections and the anisotropy factor are computed using the Mie theory. Figure 4(a) compares the $n(\lambda)$ values estimated using the Henyey-Greenstein, the modified Henyey-Greenstein approximation with those obtained using the Mie phase function. Both the H-G and the H-Gm functions overestimate the values of $n(\lambda)$ with the H-G approximation showing better agreement with the exact Mie values. From figure 4(b), it is seen that the H-G approximation gives values with less than 1.2% deviation over the wavelength range considered while the H-Gm approximation leads to less than 3% error. For the estimation of $k(\lambda)$, it can be seen from figure 4(c) and (d) that the H-G approximation again performs better. Both approximations give larger errors beyond about 800nm. Over the wavelength range considered the H-G function gives errors of less than 15% whereas with the H-Gm function the errors could be as high as 25% at some wavelengths. Figure 5 shows the performance of these approximations when used to estimate the optical constants of PMMA. Again the H-G approximation performs better than the H-Gm for estimating $n(\lambda)$. For $k(\lambda)$, the agreement with the exact Mie theory estimates are very good for both approximations.

Table 1 summarizes the results of using the RGD and the phase function approximations in terms of the average error and computing time for calculating the optical constants for 50 wavelengths. It is seen that using the exact Mie theory to calculate single particle characteristics σ_a, σ_s and g along with the H-G approximation to compute the phase function gives the lowest average error both in n(λ) and k(λ). In this case, the average error in n(λ) is 0.62% compared to 0.7% for the RGD and 2.18% when H-Gm is used. The average error in k(λ) is 4.4% compared to 23% when the RGD is used and 7.9% when the H-Gm is used. In addition, Mie theory with the HG approximation gives the greatest improvement in computing time, 73% faster than using the exact Mie calculations for the phase function compared to 10% reduction in computing time when the RGD is used and 3% reduction when the H-Gm phase function is used.

5. Discussion

In order to get a better understanding of the errors arising due to the approximations, we have to take a closer look at the optical properties to which these approximations are applied. We first look at the effect of using the RGD approximation to calculate σ_a and σ_s. In figures 6(a) and (c) the scattering and the absorption cross-section (normalised by πa^2), computed using Mie theory and RGD approximation are compared for the polystyrene sample used in this study for the wavelength range of 450 to 1320 nm. In terms of size parameters this corresponds to a range of 1.409 – 4.222. The conditions of validity of the RGD approximation is given by $|\hat{n} - 1| << 1$ and $a\kappa|\hat{n} - 1| << 1$. For the polystyrene suspension with range of size parameters considered here, the range of values for these terms are $0.1871 \le |\hat{n} - 1| \le 0.221$ and $0.2647 \le a\kappa|\hat{n} - 1| \le 0.9375$. These values do not strictly satisfy the RGD conditions. Despite this, it can be seen from figure 5(a) the

RGD values for σ_s are in good agreement with Mie theory. The percent deviation (Figure 6(b) of σ_s computed using the RGD approximation from that calculated using the Mie theory is on average about 8%. Figure 6(c) shows the normalised absorption cross-section as a function of the size parameter. It is seen that values obtained using the RGD exhibits a large deviation from the Mie theory values with deviation as higher than 40% at the lower size parameters and dropping to about 20% towards the high end on the size parameter as can be seen in figure 6(d), with the average error of around 30%. Such high errors in absorption cross-section may explain the very large deviation in the estimated $k(\lambda)$ values when the RGD approximation is used.

Next we analyse the phase functions used in this work. Figure 7 compares the different phase functions: the H-G, H-Gm and RGD approximations with the Mie phase function for different values of size parameter and g that fall in the range of particle size, refractive index and wavelength considered in this work. The parameters used in this analysis are given in Table 2. Since the phase function varies by orders of magnitude with the scattering angle, the y-axis in the plots of figure 7 are in log scale. Overall, the RGD phase function seems to be most accurate among the three phase function approximations. Specifically at the lower scattering angles where the magnitude of the phase function is the highest, the RGD phase function matches the Mie phase function very well. Thus, the reason for the large deviation in the estimation of $k(\lambda)$ appears to be solely due to the large error in the computation of σ_a and to a lesser extent on the error in σ_s using the RGD as was indicated earlier through the examination of figure 6. Based on this result, one could argue the use of the Mie theory to compute the absorption and scattering cross-section and use the RGD phase function. However, since the reduction in computation time

by using the RGD phase function is minimal, it does not lead to any advantage over the use of the exact Mie calculations.

Considering the H-G and H-Gm approximations, at first glance, it appears the H-Gm overall is a better approximation to the Mie phase function (except for the case shown in figure 7(d)). However, when we look closely, at scattering angles close to zero where the magnitude of the phase function is orders of magnitude higher than at larger angles, the H-G function is much closer (note that the y axis is in log scale) than the H-Gm function. For example in figure 7(a), the Mie phase function is about 20, the H-Gm is about 100 and the H-G value is around 10. The error in the phase function will affect the re-distribution function through χ_m^* (Eq.12) and thus the calculated values of diffuse reflectance and transmittance. Figure 8 shows the χ_m^* values obtained using the Mie, H-G and H-Gm phase functions corresponding to figure 7(a). It is seen that the H-G phase function gives a slightly better agreement with the Mie values especially for m = 1 to 3 after which the divergence from Mie values are quite high up to about m = 15. To consider the impact of the errors in χ_m^* on the calculated reflectance and transmittance, we take the conditions given by the first row in Table 2 which was used to generate the phase function plot in Figure 7(a). For this case the computed values of diffuse reflectance and transmittance are given in Table 3. It is seen that the H-G leads to a much smaller relative error in the computed values of reflectance and transmittance compared to the H-Gm. Since the optical constants are obtained by matching the experimental values of diffuse reflectance and transmittance, larger errors in these calculated values translate into larger errors in the estimated values of the optical constants.

5. Conclusions

The extraction of optical constants from multiple-scattered light using approximations to Mie theory for computing single particle characteristics was investigated by considering two suspensions of spherical particles viz. polystyrene and poly(methyl methacrylate). It was found that, for the wavelength range considered (450-1320 nm), using the exact Mie theory for calculating the absorption and scattering cross-sections, and the anisotropy parameter along with the Henyey-Greenstein approximation to calculate the phase function gave greatest improvement in terms of reduction in computing time as well as the lowest error compared to using the exact Mie theory when the reflectance and transmittance measurements are inverted to estimate the optical constants. Analysis of the Henyey-Greenstein and modified-Henyey Greenstein phase functions in the context of how the deviations of these approximations from the Mie phase function affects the redistribution function and thus the computed reflectance and transmittance measurements was carried out. The analysis suggests that errors in these computed values and thus on the estimated optical constants depend mainly on how closely the approximations match the Mie phase function at small scattering angles since the phase function has a very high magnitude in this region compared to the larger scattering angles.

Acknowledgements

This work was funded by the EPSRC through grants GR/S50441/01 and GR/S50458/01. The authors would also like to thank the Centre for Process Analytics and Control Technology (CPACT) for its support.

References

1. M. A. Velazco-Roa, and S. N. Thennadil, "Estimation of complex refractive index of polydisperse particulate systems from multiple-scattered ultraviolet-visible-near-infrared measurements " Applied Optics **46** 3730-3735 (2007).
2. A. Ishimaru, *Wave Propagation and Scattering in Random Media,* IEEE/OUP series on electromagnetic theory, (IEEE Press, New York, 1997), p.xxv,574.
3. S. A. Prahl, "The Adding-Doubling Method," in *Optical Thermal Response of Laser Irradiated Tissue*, A. J. Welch, and v. G. M. J. C., eds. Plenum Press, New York, (1995), pp. 101–129.
4. C. Bohren, and D. Huffman, "Rayleigh-Gans Theory," in *Absorption and Scattering by Small Particles*, (Wiley-VCH Germany, 2004), pp. 158-165.
5. I. G. Henyey, and J. L. Greenstein, "Diffuse Radiation in the Galaxy," The Astrophysical Journal **85**, 70-83 (1941).
6. D. Toublanc, "Henyey-Greenstein and Mie phase functions in Monte Carlo radiative transfer computations," Applied Optics **35**, 3270 - 3274 (1996).
7. W. M. Cornette, and J. G. Shanks, "Physically reasonable analytic expression for the single-scattering phase function," Applied Optics **31**, 3152-3160 (1992).
8. M. Kerker, "Rayleigh-Debye scattering," in *The scattering of Light and other Electromagnetic Radiation*, L. E. M., ed. (Academic Press, New York, 1970), pp. 414-486.
9. W. J. Wiscombe, "The delta-M method: Rapid yet accurate radiative flux calculations for strongly asymmetric phase functions," Journal of Atmospheric Sciences **34**, 1408-1422 (1977).
10. J. H. Joseph, and W. J. Wiscombe, "The Delta-Eddington Approximation for Radiative Flux Transfer," Journal of the Atmospheric Sciences **33**, 2452-2459 (1976).

11. K. N. Liou, "Approximations for radiative transfer," in *An Introduction to Atmospheric Sciences*, (Academic Press, San Diego, California USA, 2002), pp. 310-313.

12. D. Segelstein, "The Complex Refractive Index of Water," University of Missouri, Kansas City, (1981).

13. N. G. Sultanova, I. D. Nikolov, and C. D. Ivanov, "Measuring the refractometric characteristics of optical plastics," Optical and quantum electronics **35**, 21-24 (2003).

List of Figures:

Figure 1. Complex refractive index, $m(\lambda) = n(\lambda) + ik(\lambda)$ of PMMA microspheres (a) Real part, $n(\lambda)$, and (b) imaginary part, $k(\lambda)$.

Figure 2. Comparison between the complex refractive index estimated using the RGD approximation and the Mie theory for polystyrene. (a) Real part, n, (b) Percent relative error, $\Delta n = \left| n_{mie} - n_{RGD} \right| / n_{mie} * 100$, (c) Imaginary part, k. (d) Percent relative error, $\Delta k = \left| k_{mie} - k_{RGD} \right| / k_{mie} * 100$.

Figure 3. Complex refractive index of PMMA computed using Mie theory and the RGD approximation (a) real part $n(\lambda)$, and (b) imaginary part $k(\lambda)$.

Figure 4. Comparison between the optical constants estimated using the Mie phase function, the H-G and the H-Gm approximation for polystyrene. (a) n(λ). (b) Percent relative error $\Delta n = \left| n_{mie} - n_{HG(or\ HGm)} \right| / n_{mie} * 100$. (c) k(λ). (d) Percent relative error, $\Delta k = \left| k_{mie} - k_{HG(or\ HGm)} \right| / k_{mie} * 100$.

Figure 5. Comparison between the optical constants estimated using the Mie phase function, the H-G and the H-Gm approximation for PMMA. (a) n(λ) and (b) k(λ).

Figure 6. (a) Comparison between normalised scattering cross-section computed by Mie theory and the RGD approximation. (b) Percent relative error in σ_s (c) Comparison between the normalised absorption cross-section computed by Mie theory and the RGD approximation. (d) Percent relative error in σ_a.

Figure 7. Comparison between phase functions computed using Mie, RGD, HG, HGm, for particles of radius, a = 0.225 μm. (a) x = 4.1432, g = 0.86 and λ = 450 nm. (b) x = 3.1731, g = 0.8 and λ = 589 nm. (c) x = 2.1238, g = 0.69, and λ = 880 nm. (d) x = 1.5574, g = 0.44, and λ = 1200 nm.

Figure 8. Expansion coefficients, χ_n^*, computed using the δ-M method to compute the re-distribution function of the Mie, HG, and mHG phase function.

List of Tables:

Table 1. Perfromance comparison for the estimation of the optical constants using Mie theory, RGD approximation, Mie theory combined with HG, and HGm approximation for the phase function.

Table 2. Data used to compute the different phase functions shown in Figure 7.

Table 3. Comparison between total diffuse reflectance, R, and transmittance, T computed by the ADD method using Mie, HG and HGm phase functions.

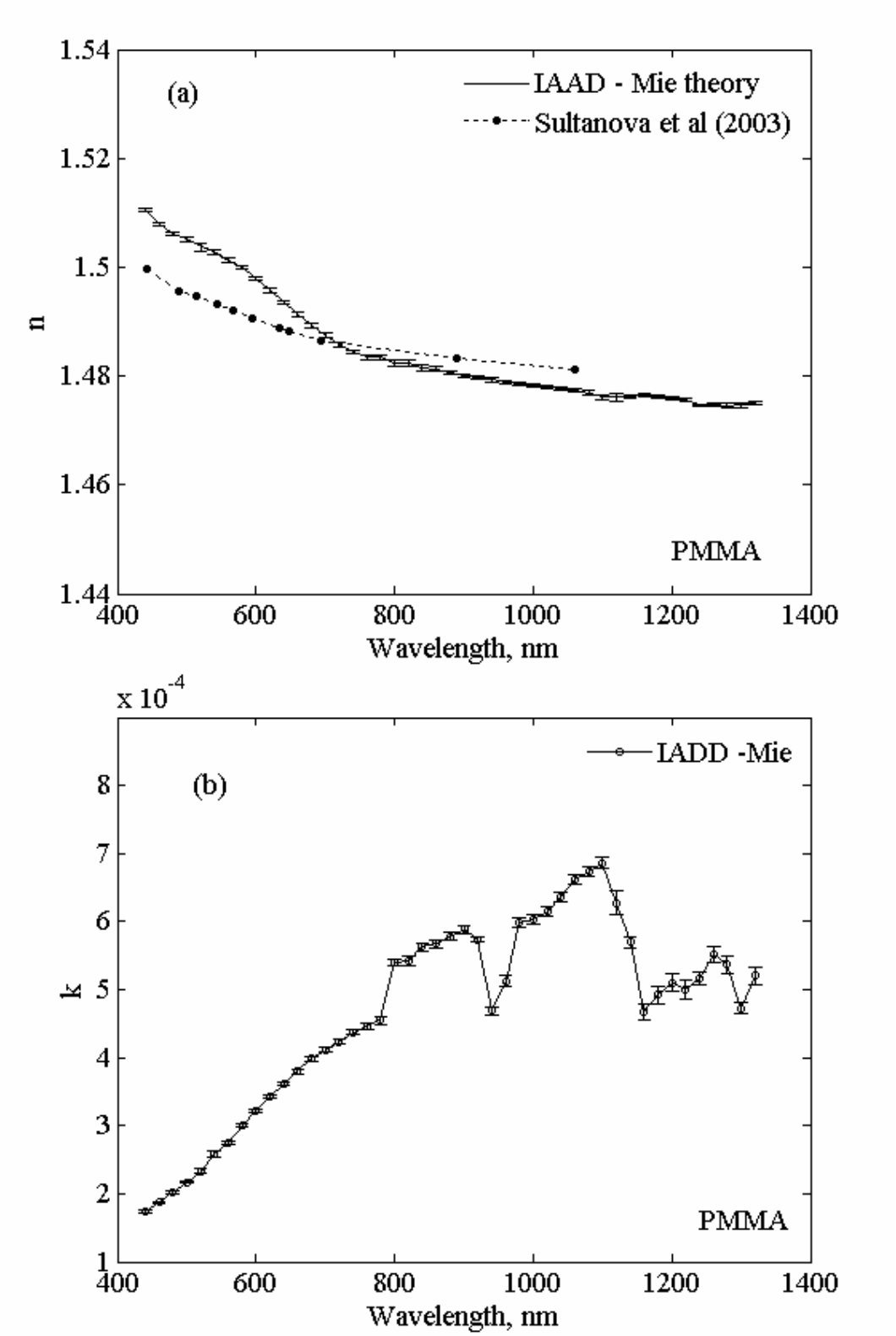

Figure 1. Complex refractive index, $m(\lambda) = n(\lambda) + ik(\lambda)$ of PMMA microspheres (a) Real part, $n(\lambda)$, and (b) imaginary part, $k(\lambda)$.

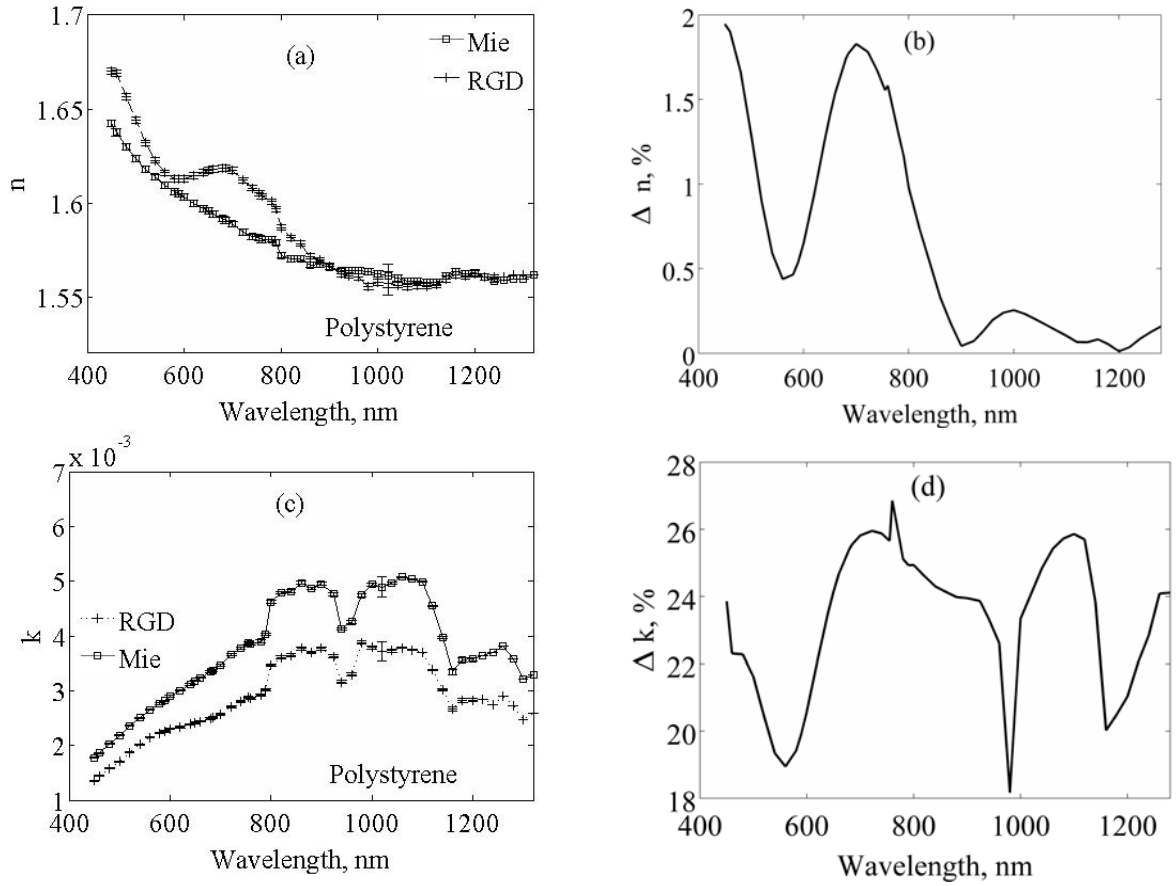

Figure 2. Comparison between the complex refractive index estimated using the RGD approximation and the Mie theory for polystyrene. (a) Real part, n, (b) Percent relative error, $\Delta n = \left|n_{mie} - n_{RGD}\right| / n_{mie} * 100$, (c) Imaginary part, k. (d) Percent relative error, $\Delta k = \left|k_{mie} - k_{RGD}\right| / k_{mie} * 100$.

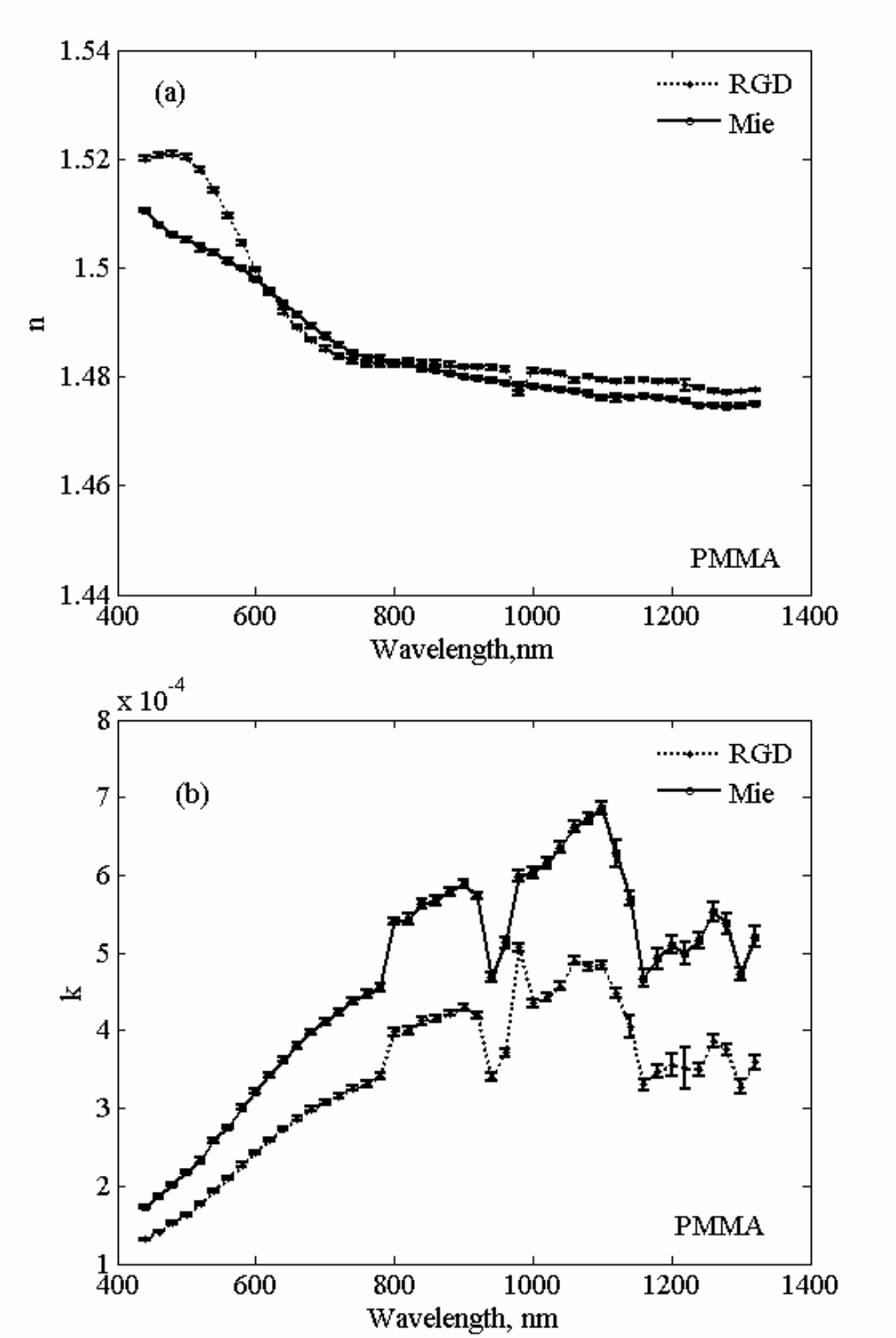

Figure 3. Complex refractive index of PMMA computed using Mie theory and the RGD approximation (a) real part $n(\lambda)$, and (b) imaginary part $k(\lambda)$.

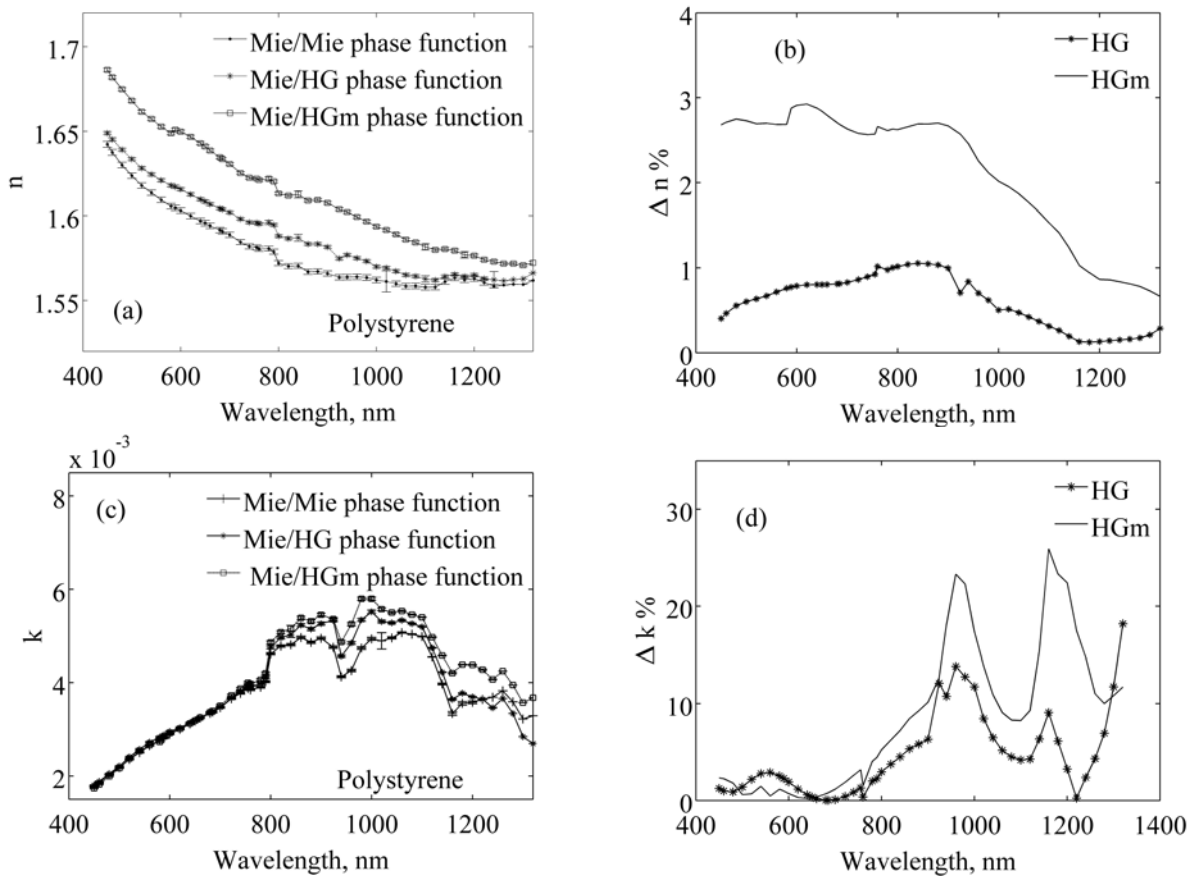

Figure 4. Comparison between the optical constants estimated using the Mie phase function, the H-G and the H-Gm approximation for polystyrene. (a) n(λ). (b) Percent relative error $\Delta n = \left| n_{mie} - n_{HG(or\ HGm)} \right| / n_{mie} * 100$. (c) k(λ). (d) Percent relative error, $\Delta k = \left| k_{mie} - k_{HG(or\ HGm)} \right| / k_{mie} * 100$.

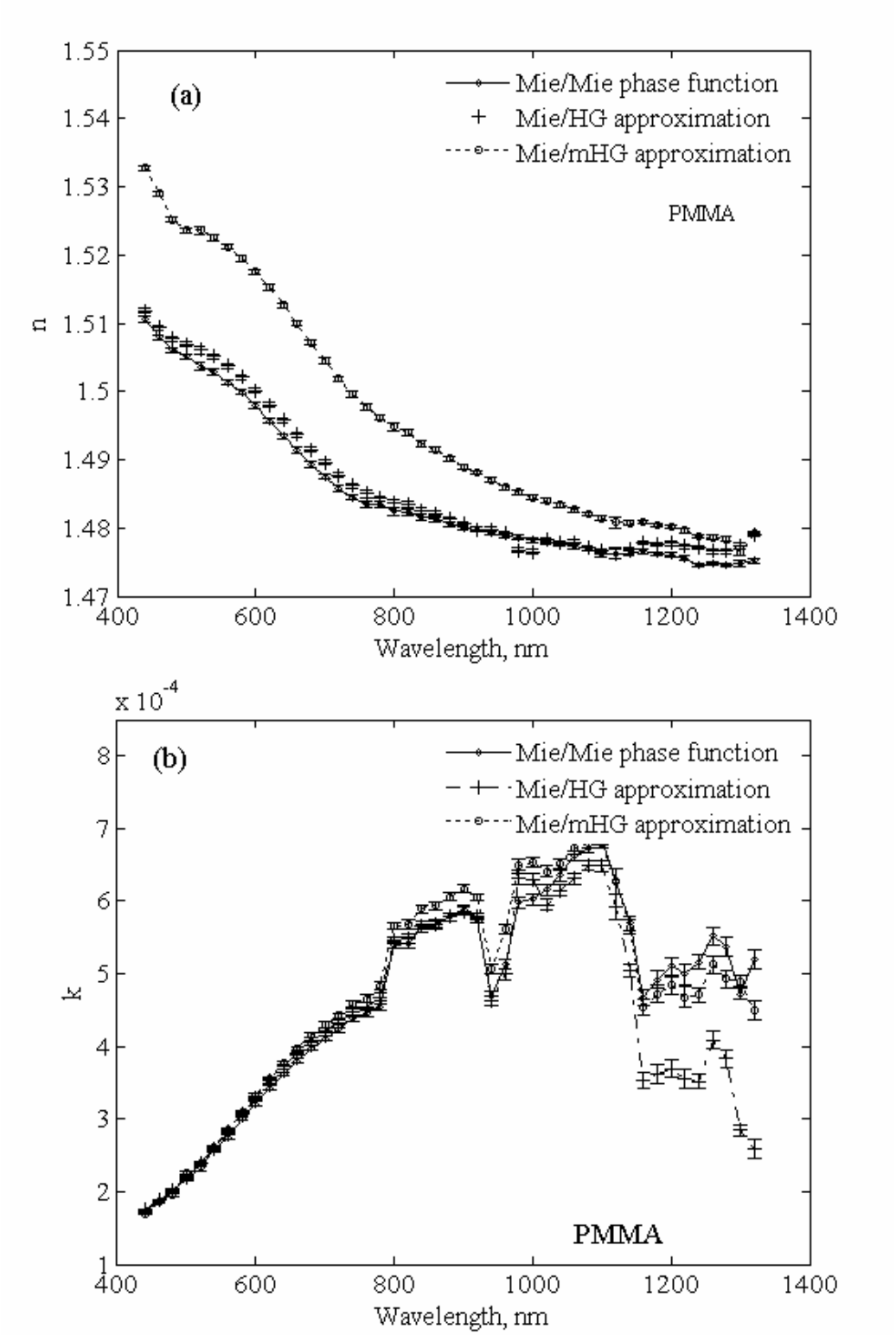

Figure 5. Comparison between the optical constants estimated using the Mie phase function, the H-G and the H-Gm approximation for PMMA. (a) n(λ) and (b) k(λ).

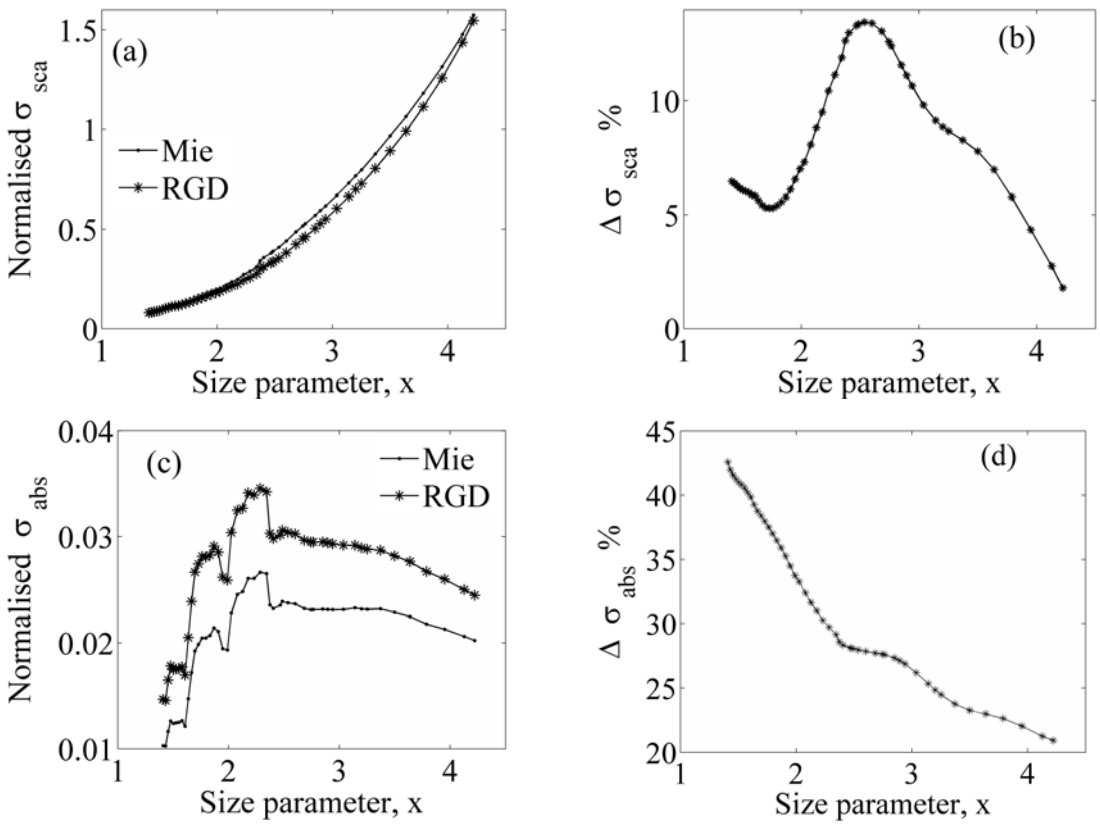

Figure 6. (a) Comparison between normalised scattering cross-section computed by Mie theory and the RGD approximation. (b) Percent relative error in σ_s (c) Comparison between the normalised absorption cross-section computed by Mie theory and the RGD approximation. (d) Percent relative error in σ_a.

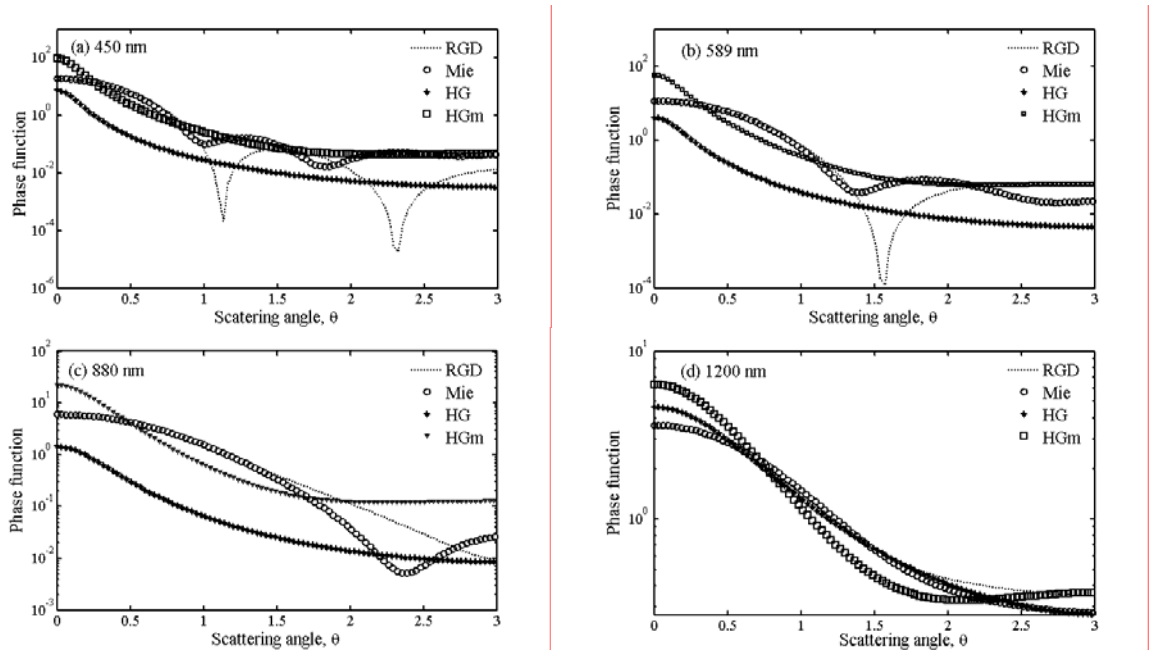

Figure 7. Comparison between phase functions computed using Mie, RGD, HG, HGm, for particles of radius, a = 0.225 μm. (a) x = 4.1432, g = 0.86 and λ = 450 nm. (b) x = 3.1731, g = 0.8 and λ = 589 nm. (c) x = 2.1238, g = 0.69, and λ = 880 nm. (d) x = 1.5574, g = 0.44, and λ = 1200 nm.

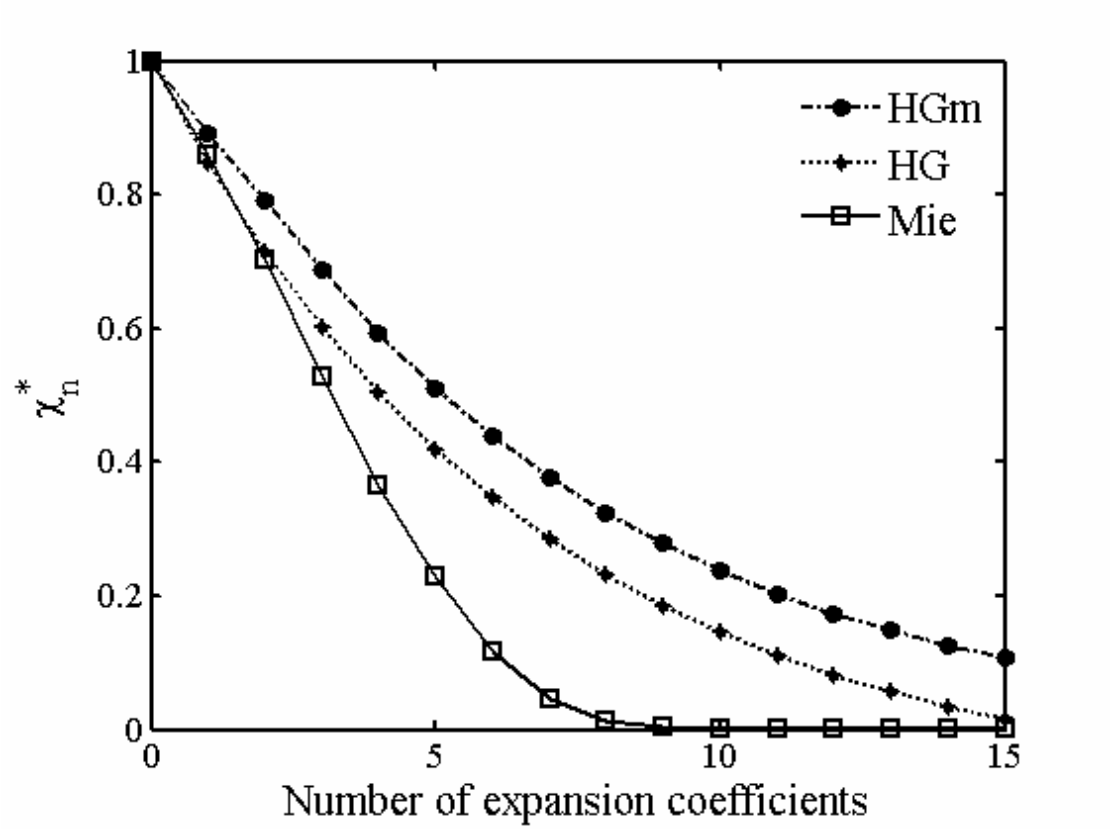

Figure 8. Expansion coefficients, χ_n^*, computed using the δ-M method to compute the re-distribution function of the Mie, HG, and mHG phase function.

Method	% Average error		Computing time (min:s)	% Decrease in the computing time
	n(λ)	k(λ)		
Mie	-	-	45:09	-
RGD	0.7	23	41:00	10
Mie/HG	0.6	4.4	13:50	73
Mie/HGm	2.2	7.9	43:48	3

Table 1. Perfromance comparison for the estimation of the optical constants using Mie theory, RGD approximation, Mie theory combined with HG, and HGm approximation for the phase function.

λ (nm)	g	$m_r = \frac{n_p + k_p i}{n_w + k_w i}$	$x = \frac{a2\pi}{\lambda_o}$
450	0.86	1.2221+0.0013i	4.1432
589	0.80	1.2033+0.0021i	3.1731
880	0.69	1.1836+0.0037i	2.1238
1200	0.44	1.1859+0.0027i	1.5574

Table 2. Data used to compute the different phase functions shown in Figure 7.

	Mie	HG		mHG	
			%Abs. Error		%Abs. Error
R	0.2751	0.2814	2.3	0.2398	12.8
T	0.4659	0.4614	1.0	0.5192	6.6

Table 3. Comparison between total diffuse reflectance, R, and transmittance, T computed by the ADD method using Mie, HG and HGm phase functions.